

# The Effect of long-range interactions on the dynamics and statistics of 1D Hamiltonian lattices with on-site potential

H. Christodoulidi<sup>1</sup>, T. Bountis<sup>2</sup>, L. Drossos<sup>3</sup>

<sup>1</sup>Research Center for Astronomy and Applied Mathematics  
Academy of Athens, Athens, Greece

University of Patras, GR-26500 Patras, Greece

<sup>2</sup>Department of Mathematics, Nazarbayev University,  
Astana, Republic of Kazakhstan

<sup>3</sup>High Performance Computing Systems and Distance Learning Lab,  
Technological Educational Institute of Western Greece, Greece

December 3, 2024

## Abstract

We examine the role of long-range interactions on the dynamical and statistical properties of two 1D lattices with on-site potentials that are known to support discrete breathers: the Klein-Gordon lattice which includes linear dispersion and the Gorbach-Flach lattice, which shares the same on-site potential but its dispersion is purely nonlinear. In both models we observe that the maximal Lyapunov exponent  $\lambda$  saturates to a positive value as the number of particles  $N$  increase, while under the implementation of long-range interactions  $\lambda$  scales as  $N^{-0.12}$  in the Klein-Gordon model and  $N^{-0.27}$  in the Gorbach-Flach, suggesting an approach to integrable behavior towards the thermodynamic limit. Furthermore, their non-Gaussian momentum distributions are distinctly different from those of the FPU model.

## 1 Introduction

In recent years there has been great interest in many-particle systems whose components interact via long-range forces [1, 2, 3, 4, 5, 6, 7, 8, 9, 10]. Such models exhibit various forms of organization, such as synchronization, collective chaos, long-living quasi-stationary states and often, even a global decrease of chaos as the number of particles increases with constant energy per particle  $\varepsilon = E/N$ . An extensively studied Hamiltonian model of this type with long-range forces is the so-called Mean Field Hamiltonian (HMF), which is composed by  $N$  identical particles lying on a ring [1, 2, 3]. In this globally coupled system each particle interacts equally with all the others, independently of the topological distance among the sites. An important result of these studies [1, 2] is that the maximal Lyapunov exponent scales with the degrees of freedom like  $\lambda \sim N^{-1/3}$ , suggesting a non-ergodic behavior towards the thermodynamic limit.

More recently, the authors of the present paper, together with C. Tsallis, studied a long-range interaction generalisation of the one-dimensional (1D) Fermi-Pasta-Ulam (FPU)  $\beta$ -model [11], by introducing a quartic interaction coupling constant that decays as  $1/r^\alpha$  ( $\alpha \geq 0$ ), with  $\alpha \rightarrow \infty$  corresponding to the nearest-neighbor FPU model [4]. Through molecular dynamics, it was shown that: (i) For  $\alpha \geq 1$  the maximal Lyapunov exponent is finite and positive for increasing number of particles  $N$ , whereas, for  $0 \leq \alpha < 1$ , it asymptotically decreases as a power law in  $N$ . (ii) The distribution of time-averaged velocities is Gaussian for  $\alpha$  large enough, whereas it becomes a  $q > 1$ -Gaussian, when  $0 \leq \alpha < 1$ , thus leading for  $\alpha$  small enough to a crossover from  $q$ -statistics [20, 21, 22, 23] to Boltzmann-Gibbs (BG) thermostatics as time increases.

In a subsequent paper, the same FPU model was revisited introducing long-range interactions (LRI) in both the quadratic and quartic parts of the potential, via two independent exponents  $\alpha_1$  and  $\alpha_2$ . It was demonstrated that weak chaos, in the sense of decreasing Lyapunov exponents and  $q$ -Gaussian probability density functions (pdfs), occurs only when long-range interactions are included in the quartic part [5], while, under certain conditions, these pdfs are found to persist as  $N \rightarrow \infty$ . On the other hand, when LRI are imposed only on the quadratic part, strong chaos and purely Gaussian pdfs are always obtained. In fact, in the extremal case where phonons are completely absent [9], the FPU system under LRI exhibits the same ‘non-ergodic’ behavior, with  $\lambda \sim N^{-1/3}$  towards the thermodynamic limit, as in the HMF model.

It is important to recall, of course, that the HMF and FPU models are characterized by translational invariance. Thus, in the present paper, we investigate whether any of the above phenomena also occur in Hamiltonian 1D lattices possessing on-site potentials. As is well-known, such systems typically exhibit localized oscillations called discrete breathers. It would be challenging to extend previous studies of the impact of LRI on the dynamics and statistics of such models. To this end, we focus here on two 1D Hamiltonians with on-site potentials, namely, the Klein-Gordon (KG) and Gorbach-Flach (GF) models [12, 13]. Inspired by our previous studies, we add to the linear dispersion of these models quartic interactions, and proceed to investigate their effect on the dynamics, by computing Lyapunov exponents, and statistics, by analyzing their momentum distributions for increasingly  $N$  values.

## 2 The KG and GF Hamiltonians with on site potential

We shall consider two types of 1D Hamiltonian lattices which share the same on-site potential but differ in the degree of their dispersive terms. The first one is the classic Klein-Gordon (KG) lattice, with quadratic and quartic on site potential and *linear* dispersion terms, described by the Hamiltonian:

$$H^{KG}(p, x) = \sum_n \frac{1}{2}p_n^2 + \frac{1}{2}x_n^2 + \frac{1}{4}x_n^4 + \frac{C}{2}(x_{n+1} - x_n)^2. \quad (1)$$

The second one is the Gorbach-Flach model (GF) [12] consisting of  $N$  coupled oscillators, with the same KG on-site potential, but with *only quartic* interactions among its nearest-neighbor sites,

$$H^{GF}(p, x) = \sum_n \frac{1}{2}p_n^2 + \frac{1}{2}x_n^2 + \frac{1}{4}x_n^4 + \frac{C}{4}(x_{n+1} - x_n)^4, \quad (2)$$

and is hence free from linear dispersion. In both systems  $p_n$  and  $x_n$  represent the canonical conjugate pairs of momenta and positions respectively, satisfying periodic boundary conditions  $x_0 = x_N, x_{N+1} = x_1$ . In short, the two Hamiltonians (1) and (2) have the form:

$$H(p, x) = \sum_n \frac{1}{2}p_n^2 + V(x_n) + W(x_{n+1} - x_n) = E \quad (3)$$

where  $E$  is the total energy. By  $V(x)$  we denote the so-called ‘hard’ on-site potential  $\frac{1}{2}x^2 + \frac{1}{4}x^4$ , present in both systems, while  $W(x)$  denotes the potential functions  $W^L(x) = \frac{C}{2}x^2$  and  $W^N(x) = \frac{C}{4}x^4$  describing linear and nonlinear coupling in KG and GF, respectively.

As is well known, these systems can support localized periodic oscillations called *discrete breathers*, centered about any one of their sites [14, 15, 16, 17]. The simplest ones among them are easy to find, by judiciously exciting a single site, provided their frequency lies outside the linear frequency spectrum of the lattice. If they are stable, their approximate form will be preserved in time, while if they are unstable they will eventually collapse and share their energy with all particles of the lattice. In Fig. 1 we display two examples of such breathers for the KG and GF models studied in this paper.

### 2.1 Energy spreading after single-site excitations

Let us now focus on the effect of linear and nonlinear dispersion in the dynamics of the KG and GF lattices separately, following a single-site excitation of the central particle by a momentum shift of

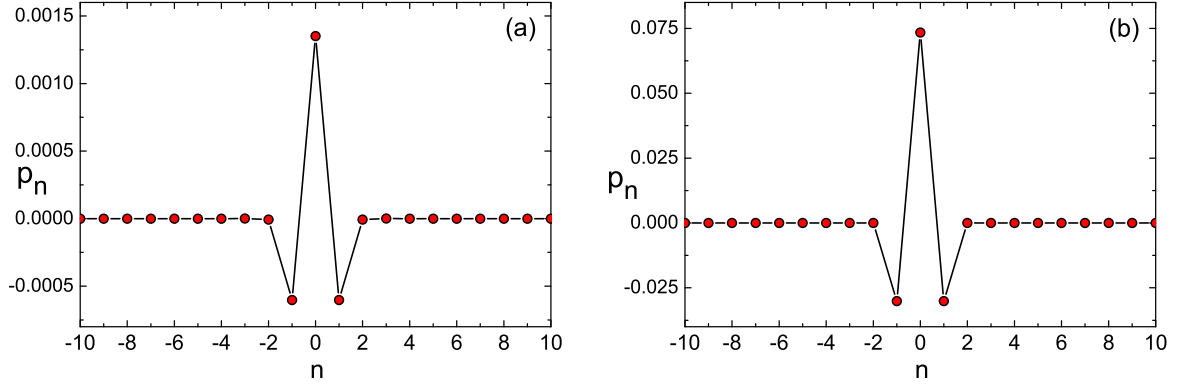


Figure 1: A breather-like profile obtained a short time after a single-site excitation ( $n = 0$ ) in (a) the Klein-Gordon model and (b) the Gorbach-Flach model, for  $N = 256$  particles.

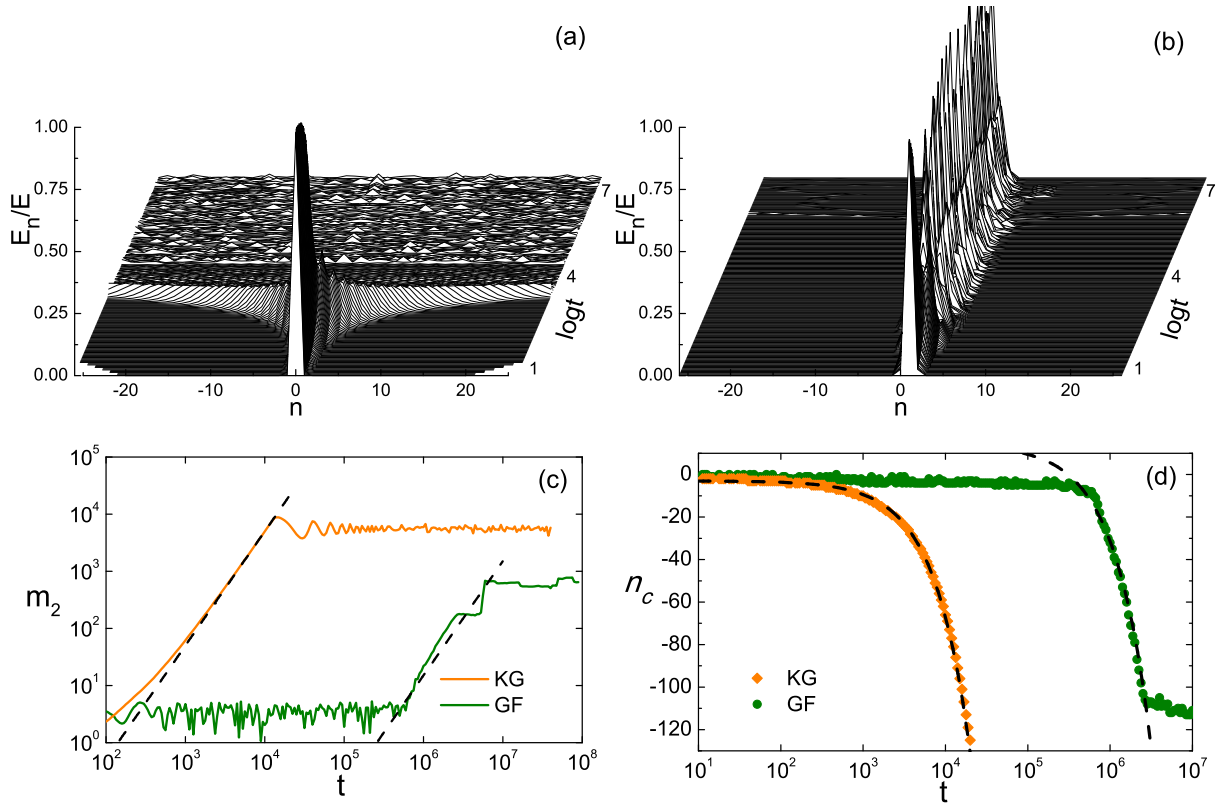


Figure 2: The temporal evolution of the normalized on-site energies in (a) the classical Klein-Gordon model and (b) the Gorbach-Flach model. We plot the time evolution of (c) the second moment  $m_2$  and (d) the borderline separating excited from non-excited particles in both models.

$p_0(0) = A$ . Due to the absence of linear dispersion in the latter model, it is clear from Fig. 2 that the GF breather is significantly more robust.

Energy spreading can be efficiently monitored by the temporal evolution of the on-site energies  $E_n$ , given by

$$E_n = \frac{1}{2}p_n^2 + \frac{1}{2}x_n^2 + \frac{1}{4}x_n^4 \quad ,$$

as shown in Fig.2(a) and (b) for both models. We consider a KG lattice with coupling constant  $C = 0.01$  and  $p_0(0) = 0.01$  and a GF lattice with  $C = 1$  and  $p_0(0) = 0.2$ , with  $N = 256$  particles. Comparing the linear and the nonlinear dispersion in the first two panels of Fig.2, we observe that the KG model quickly experiences a resonant energy transfer, in contrast to the GF model where localization persists for very long times and energy propagation is much less pronounced. The near absence of diffusion in the latter case can be attributed to the lack of a linear frequency band and hence the absence of breather-phonon resonances.

To quantify the energy diffusion for single-site or wave-packet excitations we applied two different indicators. The first indicator is the second moment, defined as

$$m_2 = \sum_n n^2 \frac{E_n}{E},$$

which we plot in Fig.2(c) following an excitation of only the 0-th particle. The second indicator is the movement of the borderline particle  $n_c$  on the propagating front, separating the vibrating particles from the non-excited ones (Fig.2(d)). As we see in Fig.2(c) the second moment increases in time as  $m_2 \propto t^2$  for both models, even though in the GF model localization persists to a much larger extent. Fig.2(d) clearly suggests that the temporal evolution of the borderline particle evolves as  $n_c \propto t$ .

The two diffusion indicators are approximately related by  $m_2(t) \propto n_c^2(t)/3$ , which is approximately equipartitioned among the  $n_c$  particles, i.e.  $E_n/E \simeq n_c^{-1}$ , so that  $m_2 \simeq n_c^{-1} \sum_{n=1}^{n_c} n^2 \simeq n_c^2/3$ . Thus, both indicators imply a *ballistic* propagation of the energy in KG which completely delocalizes the energy after short times.

The ultimate saturation of  $m_2$  is due to the finite  $N$ -size of the models and therefore the boundaries are eventually reached. Note that, in the GF model, the second moment and the  $n_c$  propagation do reveal a limited amount of energy transfer, which, however, does not essentially affect the localization.

## 2.2 Energy spreading under long-range interactions

Let us note now that our KG and GF 1D Hamiltonians, as they appear in (1) and (2), involve nearest-neighbor interactions. It would be interesting to ask, therefore, how do their dynamical and statistical properties change if we extend the range of interactions and introduce forces that decay with distance according to  $1/r^\alpha$ . This implies an appropriate modification of the potential function  $W(x)$ . The LRI-Hamiltonian then becomes:

$$H(p, x) = \sum_n \left( \frac{1}{2}p_n^2 + V(x_n) + \frac{1}{2\tilde{N}} \sum_m \frac{W(x_m - x_n)}{r_{n,m}^\alpha} \right), \quad (4)$$

where  $r_{n,m} = \min\{|n - m|, N - |n - m|\}$  defines the minimum topological distance between the particles  $n$  and  $m$  and  $\tilde{N} = 1/N \sum_{n,m} 1/r_{n,m}^\alpha$  provides a rescaling factor that maintains extensivity in the Hamiltonian (4), i.e. that all its parts grow  $\propto N$ .

In the remainder of the paper we focus only on the particular  $\alpha = 0$  case, for which, the LRI-Hamiltonian (4) simplifies to:

$$H(p, x) = \sum_n \left( \frac{1}{2}p_n^2 + V(x_n) + \frac{1}{2\tilde{N}} \sum_m W(x_m - x_n) \right), \quad (5)$$

with  $\tilde{N} = N - 1$ . By *KG-LRI* and *GF-LRI* we refer to the Klein-Gordon and the Gorbach-Flach models with long-range interaction, as described by the Hamiltonian (5) for appropriate  $W(x)$  potential functions.

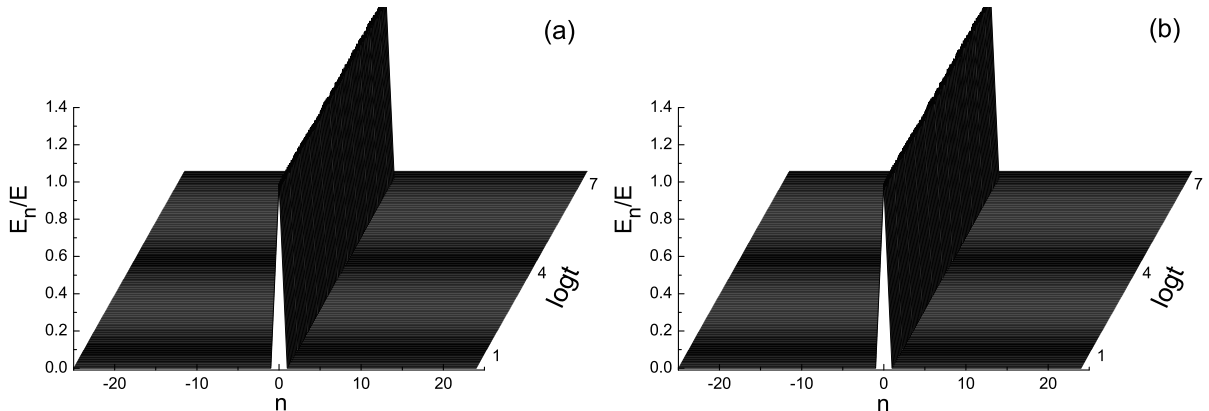


Figure 3: Energy spreading for (a) the Klein–Gordon and (b) the Gorbach–Flach models with long–range interactions. All parameter values are the same with Fig.2(a) and (b) respectively.

One interesting observation concerning breather generation and collapse can be made by imposing again one–site excitations of appropriate magnitude to our new lattices with Hamiltonians of the form (5). As has been convincingly shown in [18], LRI destroy the *strong localization profile* of discrete breathers, in the sense that, the exponential tails of the breather become algebraic. On the other hand, concerning *energy localization*, our results show that the implementation of LRI is not only non–catastrophic; it can actually be beneficial!

We repeat the calculations of Fig.2 for the long–range case, keeping all parameters the same and we find that the energy remains localized for very long times, without any evidence of energy diffusion in both KG and GF models. For example, in Fig.3 we observe that a single–site excitation ( $n = 0$ ) results in a remarkably stable breather–like solution which shows no sign of collapse, even after very long times. One reason for this, regarding the KG–LRI model, is the monotonical vanishing of the width of the linear spectrum as the LRI index  $\alpha$  in (4) goes to zero, hence breather–phonon resonances become more and more rare [5, 7]. In the GF case, however, such resonances are absent from the outset.

The equations of motion for our Hamiltonian (5) become:

$$\ddot{x}_n = -x_n - x_n^3 - \frac{C}{2N} \sum_m (x_m - x_n)^p, \quad (6)$$

where  $p = 1$  for KG and  $p = 3$  for GF with LRI. A careful inspection of (6) shows that all particles share an ‘identical’ equation of motion, where  $x_n$  interacts equally with all other particles. This means that if all particles share the same initial condition, e.g.  $x_n(0) = c$  with zero momenta, the system would be described by the one–degree of freedom equation  $\ddot{x}_n = -x_n - x_n^3$ , in other words, all positions  $x_n(t)$  would be equal at all times. Consequently, it can be seen that a single–site excitation  $x_0(0) \neq 0$ , with  $x_n(0) = 0$  for all  $n \neq 0$  (and zero momenta), reduces the equations (6) to a two–degree of freedom system.

This is of course true in the particular case of *all-to-all couplings* with  $\alpha = 0$  among the particles. Still, it would be interesting to pursue this case further, and examine in more detail the dynamical and statistical behavior of these models for a random choice of initial conditions and gradually increase the energy per particle and/or the system size.

### 3 Dynamics under long–range interactions with $\alpha = 0$

As explained in the Introduction, in the case of translationally invariant Hamiltonians like the FPU and HMF models, LRI has important implications regarding their dynamical and statistical behavior towards the thermodynamic limit. In particular, for  $0 \leq \alpha < 1$ , maximal Lyapunov exponents  $\lambda$  exhibit

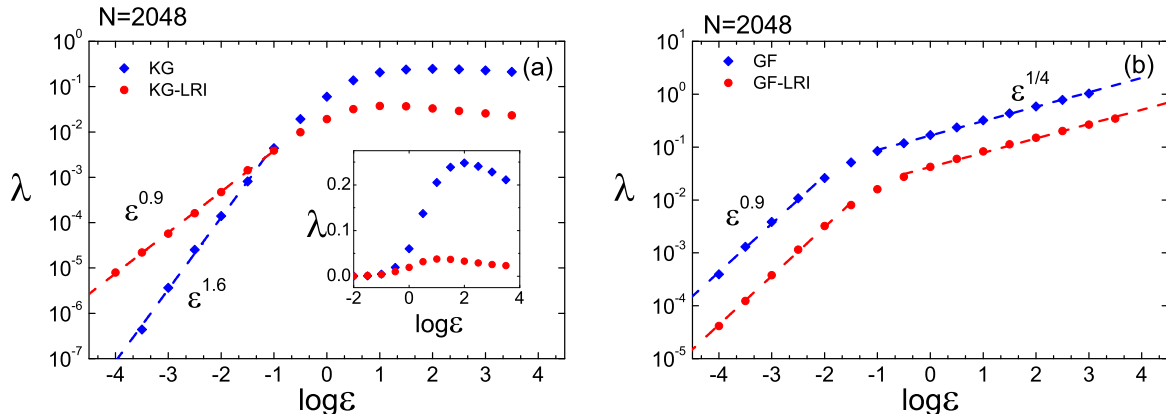


Figure 4: The maximal Lyapunov exponent  $\lambda$  for increasing energy values of  $\varepsilon$  and fixed number of particles  $N = 2048$ . (a) The classical KG model (blue diamonds) and the KG model with LRI (red circles). Inset: a closer look to the  $\lambda$  values at high energies. (b) The GF model (blue diamonds) and the GF model with LRI (red circles)

saturation phenomena as the energy per particle  $\varepsilon$  increases, while they tend to decrease to zero with increasing  $N$ .

On the other hand, LRI are also associated with a change in the thermostatics, since, for  $0 \leq \alpha < 1$ , momentum probability distributions (pdfs) deviate from Gaussians and approach  $q > 1$ -Gaussians, characterized by long tails and algebraic power laws [4, 5]. We have attributed to this kind of regularization the term “weak chaos”, as opposed to “strong chaos” associated with non-decreasing  $\lambda$  and Gaussian pdfs related to exponential decay of correlations.

Let us now investigate whether similar effects occur in the present models when we estimate maximal Lyapunov exponents as functions of  $\varepsilon, N$  and momentum pdfs as they evolve to a stationary shape, starting as always from initial momenta drawn randomly from a uniform distribution.

### 3.1 Small and large energy limits

As is well-known, the maximal Lyapunov exponent  $\lambda$  measures the strength chaos in the dynamics of nonlinear systems. Thus, we proceed to systematically calculate the maximal Lyapunov exponent  $\lambda$  for our KG and GF models, as well as for their corresponding long-range cases, when the energy per particle  $\varepsilon$  is gradually increased. We remark that an interesting behavior of the maximal Lyapunov exponent is observed, as illustrated here in Fig.4 for  $N = 2048$  particles with strong couplings, i.e.  $C = 1$ .

In the zero energy limit, both the classical KG model and the KG with LRI exhibit a power-law dependence on the energy  $\varepsilon$ , namely  $\lambda_{KG} \sim \varepsilon^{1.6}$  and  $\lambda_{KG}^{LRI} \sim \varepsilon^{0.9}$  respectively (Fig.4(a)). In the KG model the steeper decay of  $\lambda$ , which occurs when  $\varepsilon \rightarrow 0$ , is due to the fact that  $W(x)$  is dominated by the nonlinearity  $\frac{1}{4}x_n^4$ . This, however, does not happen in the KG-LRI case, where due to the flattening of  $W(x)$  the linear terms and nonlinearity  $\frac{1}{4}x_n^4$  balance.

As we now progressively increase the energy, the maximal Lyapunov exponent reaches its maximum value for  $\varepsilon = \varepsilon_{cr}$ , while it decreases again as  $\varepsilon \rightarrow \infty$  for both Hamiltonians  $H_{KG}$  and  $H_{KG}^{LRI}$ . This interesting phenomenon is due to the fact that the nonlinearity  $1/4x_n^4$  scales with the system’s energy. In particular, when  $\varepsilon \rightarrow \infty$  the quartic on-site potential drives the system towards the *uncoupled Hamiltonian system*:

$$H_0 = \sum_n \frac{1}{2}p_n^2 + \frac{1}{2}x_n^2 + \frac{1}{4}x_n^4$$

of  $N$  self-driven particles, which causes, above a critical value  $\varepsilon_{cr}$ , the decrease of the maximal Lyapunov exponent.

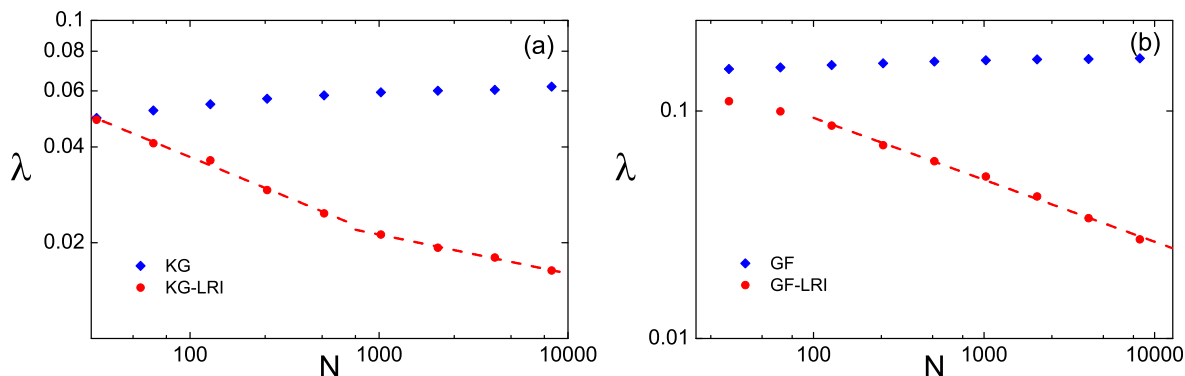


Figure 5: The maximal Lyapunov exponent for an increasing number of particles  $N$ . (a) KG (blue) diamonds and KG–LRI (red) circles. (b) GF (blue) diamonds and GF–LRI (red) circles.

Let us now ask the same questions for the classical GF model and its corresponding long–range case. Here, the energy spreading among the particles is only due to higher–order couplings, which scale with the energy and thus play a leading role in the system’s behavior. Thus, in the zero energy limit we find  $\lambda_{GF}, \lambda_{GF}^{LRI} \sim \varepsilon^{0.9}$  (see Fig.4(b)), similarly with the KG–LRI system. In the large energy limit, on the other hand, we find that  $\lambda_{GF}, \lambda_{GF}^{LRI} \sim \varepsilon^{0.27}$ . Evidently, there is a similar behavior in terms of the maximal Lyapunov exponent in the GF and the GF–LRI models, at all energy ranges, contrary to their KG counterparts.

As a final remark, we would like to stress that when LRI are applied to a model of the form (3), the coupling terms in  $W(x)$  are smoothed out. In KG the “flattening” of the terms  $1/2(x_{n+1} - x_n)^2$  drives the system faster towards an uncoupled Hamiltonian system, while in the GF model the “flattening” of the terms  $1/4(x_{n+1} - x_n)^4$  reduces the maximal Lyapunov exponent to lower values. It also worth mentioning that the behavior of the maximal Lyapunov exponent  $\lambda \sim \varepsilon^{1/4}$  in the GF and GF–LRI models for  $\varepsilon \gg 1$  is reminiscent of the Fermi–Pasta–Ulam– $\beta$  model [19], which includes both types of coupling terms, namely  $1/2(x_{n+1} - x_n)^2$  and  $1/4(x_{n+1} - x_n)^4$ .

### 3.2 Approaching an “integrable” behavior in the thermodynamic limit

A surprising result awaits us regarding the behavior of the maximal Lyapunov exponent when the number of particles  $N$  grows to larger and larger values. Indeed, when we take  $\varepsilon = 1$  and compare the behavior of  $\lambda$  in the classical and long–ranged KG and GF models, we find a striking difference between short and long interactions. As Fig. 5(a),(b) clearly show, the range of interactions has a dramatic effect on the chaotic properties of both systems: While, under short–range interactions,  $\lambda$  tends to saturate to a positive value, LRI make  $\lambda$  decrease towards zero, thus indicating that both systems become less and less chaotic as  $N$  increases.

In Fig.5(a) there are two best line fits describing the decay of  $\lambda_{KG}^{LRI}$  of the KG system: A power-law  $N^{-0.24}$  for the data up to  $N \simeq 1000$ , which slows down to  $N^{-0.12}$  for larger  $N$ . In Fig.5(b), on the other hand, the maximal Lyapunov exponent of the GF model exhibits a clear decay with  $N$ , that is found to scale as  $\lambda_{GF}^{LRI} \sim N^{-0.27}$ . At this point it is worth mentioning that the exponent 0.27 is closer to  $1/4$  than to  $1/3$ , which is the case for the HMF model [1, 2, 3] and the FPU–LRI in the absence of quadratic terms [9].

These results indicate that the implementation of LRI leads to systems that are mainly driven by their on–site potential. This is because, as we have argued, LRI renders the coupling terms in  $W(x)$  unimportant and consequently both lattices in the large  $N$  limit approach the integrable behavior of systems composed of uncoupled particles. There is, however, one distinct difference between the two models: When LRI are imposed to the KG system, the decrease of  $\lambda$  slows down for  $N > 1000$ , while it continues to decay steadily in the GF model. The reason for this difference is presently not known to

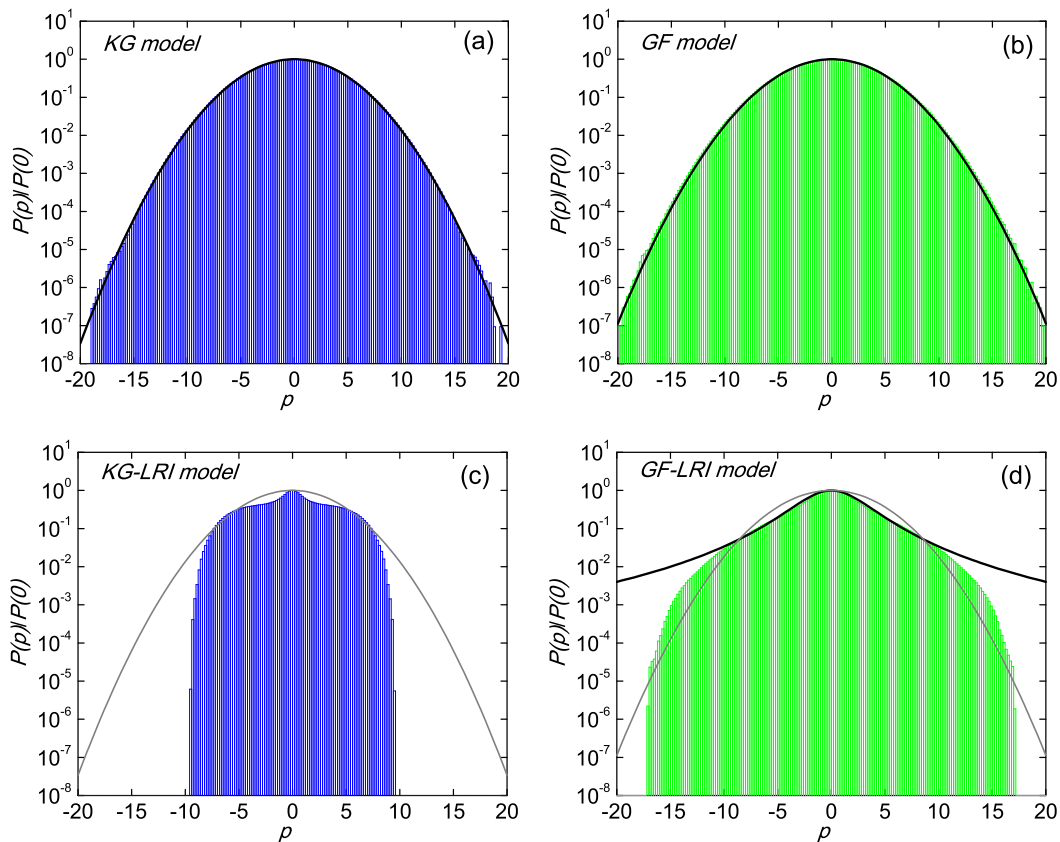


Figure 6: Time-averaged momentum distributions of 4 cases with  $N = 2048$  and  $\varepsilon = 10$  in the (a) KG, (b) GF, (c) KG-LRI and (d) GF-LRI models respectively.

us and constitutes one more interesting point that needs to be further studied in the future.

## 4 Momentum distributions of weak and strong chaos at thermal equilibrium

Finally let us focus on the statistical properties of the aforementioned systems. With initial momenta drawn randomly from a uniform distribution, as described in Section 3, we shall evaluate the momenta distributions for fixed  $N = 2048$  and  $\varepsilon = 10$ , at times long enough for the pdfs to have reached a stationary shape. As we demonstrate in Fig. 6, the resulting pdfs for short and long-range distributions are distinctly different: In the classical KG and GF models the pdfs quickly approach a Gaussian, suggesting a state of strong chaos, shown in Fig. 6(a),(b). On the other hand, when LRI are imposed, the corresponding distributions are quite far from Gaussians, as Fig. 6(c),(d) clearly show.

Interestingly, even though they are associated with dynamically weakly chaotic regimes and non-equilibrium thermodynamics, the KG and GF pdfs under LRI, are not well approximated by  $q$ -Gaussians, as we had found in our earlier studies on the FPU- $\beta$  lattice [4, 5]. This difference may be attributed to the fact that, unlike the FPU, the KG and GF models of the present paper possess on-site potentials, which break translational invariance. This suggests that the thermostatics of weak chaos in LRI 1D Hamiltonian lattices remains an open subject, that definitely merits further investigation.

## 5 Conclusions

The present study aims to elucidate the role of linear and nonlinear long-range interactions on the dynamical and statistical behavior of systems possessing on-site potentials, well known for supporting the emergence of discrete breathers. To this end, we have chosen two models, the Klein–Gordon lattice which includes a non-trivial frequency band and the Gorbach–Flach model, which contains only nonlinear coupling terms. Simple experiments of exciting only one particle show that the energy spreads under a ballistic diffusion process due to resonances in the KG model, while it remains to a large extent localized in the GF model. Still, in both cases, the presence of long-range interactions causes a dramatic change in the system’s behavior, as the initially excited particle preserves the energy to a great degree for very long-times, if not for all times. One can therefore conclude that such LRI–systems are the best candidates to search for and study a variety different kinds of localized solutions.

When more complicated initial conditions are imposed, such as the random momenta excitations of all the particles in the KG–LRI and GF–LRI models, there is an overall dynamical ‘regularization’ towards the thermodynamic limit. This regularization is quantified by a power–law decay  $N^{-\mu}$ ,  $\mu > 0$  of the maximal Lyapunov exponent  $\lambda$ , which indicates a weaker form of chaos and a possible integrable–like behavior as  $N \rightarrow \infty$ . These results are reinforced by a non–trivial statistical behavior of the corresponding momentum distributions, which however, do not fit a precise  $q$ –Gaussian shaped pdf. To this end, we believe that our findings open a variety of interesting questions, which are deferred to a future study. Notwithstanding the vast unexploited properties of systems whose components interact via long–range forces, the above results suggest a notable organized behavior, which becomes more and more regular as the degree of complexity and the number of particles increase.

## 6 Acknowledgements

The authors acknowledge interesting discussions with Professor C. Tsallis on the results of this paper. A.B. expresses his gratitude for a grant by Nazarbayev University that supported his participation to a Dynamics Days Conference at Puebla, Mexico, in November 2016, where some of the early results reported in this paper were presented. H.C. was supported by the State Scholarship Foundation (IKY) operational Program: ‘Education and Lifelong Learning–Supporting Postdoctoral Researchers’ 2014–2020, and is co–financed by the European Union and Greek national funds.

## References

- [1] C. Anteneodo, C. Tsallis, Phys. Rev. Lett. **80** 5313 (1998)
- [2] V. Latora, A. Rapisarda, S. Ruffo, Phys. Rev. Lett. **80** 692 (1998)
- [3] L.J.L. Cirto, V. Assis, C. Tsallis, Physica A **393** 286–296 (2013)
- [4] H. Christodoulidi, C. Tsallis, T. Bountis, EuroPhysics Letters EPL, **108**, 40006 (2014)
- [5] H. Christodoulidi, T. Bountis, C. Tsallis, L. Drossos, J. Stat. Mech. 123206 (2016)
- [6] G. Miloshevich, J.P. Nguenang, T. Dauxois, R. Khomeriki, S. Ruffo, Phys. Rev. E **91** 032927 (2015)
- [7] G. Miloshevich, J.P. Nguenang, T. Dauxois, R. Khomeriki, S. Ruffo, J. Phys. A: Math. Theor. **50** 12LT02 (2017)
- [8] S. Gupta, S. Ruffo, Int. J. Mod. Phys. A **32**, 1741018 (2017)
- [9] D. Bagchi, C. Tsallis, Phys. Rev. E **93** (6), 062213, (2016)
- [10] D. Bagchi, C. Tsallis, Physica A **491**, 869–873, (2018)
- [11] E. Fermi, J. Pasta, S. Ulam, Los Alamos, Report No. LA-1940, (1955)
- [12] A.V. Gorbach, S. Flach, Phys. Rev. E **72**, 056607 (2005)
- [13] P. Maniadis, T. Bountis, Phys. Rev. E **73**, 046211 (2006)
- [14] R.S. MacKay, S. Aubry, Nonlinearity **7**, 1623 (1994)

- [15] S. Flach, Phys. Rev. E **51**, 3579 (1995)
- [16] J.M. Bergamin, T. Bountis, C. Jung, J. Phys. A, Math. Gen. **33**, 8059 (2000)
- [17] J.M. Bergamin, T. Bountis, M.N. Vrahatis, Nonlinearity **15**, 1603 (2002)
- [18] S. Flach, Phys. Rev. E **58** (4), R4116–R4119 (1998)
- [19] L. Casetti, R. Livi, M. Pettini, Phys. Rev. Lett. **74** 375–378 (1995)
- [20] C. Tsallis, 1988 *Stat. Phys.* **52** 479 [First appeared as preprint in 1987: CBPF-NF-062/87, ISSN 0029-3865, Centro Brasileiro de Pesquisas Físicas, Rio de Janeiro]
- [21] M. Gell-Mann, C. Tsallis, eds., *Nonextensive Entropy - Interdisciplinary Applications* (Oxford University Press, New York, 2004)
- [22] C. Tsallis, *Introduction to Nonextensive Statistical Mechanics - Approaching a Complex World* (Springer, New York, 2009)
- [23] C. Tsallis, Contemporary Physics **55** 179-197 (2014)